JOURNAL OF APPLIED ELECTROCHEMISTRY 25 (1995) 456–461

Development of a rotating ring-disc electrode for high temperature studies in cryolite-based melts

R. S. STOJANOVIC, J. F. KUBACKI, R. DORIN, E. J. FRAZER*

CSIRO Institute of Minerals, Energy and Construction, Division of Mineral Products, P.O. Box 124, Port Melbourne, Victoria 3207, Australia

Received 2 July 1994; revised 20 September 1994

A compact rotating ring-disc electrode incorporating a molybdenum disc, gold ring and boron nitride insulator has been designed, constructed and evaluated in molten cryolite-based electrolytes at temperatures up to 1000 °C and rotation rates between 0 and 2000 rpm. The electrode design is extremely versatile and relatively maintenance free, with no visible evidence of melt leakage at the ring-insulator and disc-insulator interfaces. The operating performance of the gold-molybdenum rotating ring-disc electrode was evaluated from collection efficiency measurements based on the dissolution of the disc surface and subsequent detection of soluble species transported to the ring. The observed collection efficiency was less than the theoretical value determined from the geometry of the electrode, primarily because of noncoplanarity of the electrode surface at the working temperature. The results confirm that the electrode should be useful for mechanistic studies in high temperature molten fluoride electrolytes.

1. Introduction

Electrochemical studies in molten salt electrolytes have predominantly been carried out at stationary metal or graphite electrodes using techniques such as chronopotentiometry, cyclic voltammetry, pulse voltammetry, coulometry, and to a lesser extent, rotating disc voltammetry [1, 2]. Although these techniques allow various aspects of an electrochemical process to be characterized, they are only of limited value in the case where the overall electrochemical reaction mechanism proceeds via the formation of a chemical intermediate. The rotating ring-disc electrode (RRDE) is an extremely powerful and well established technique for studying complex chemical and electrochemical reactions in aqueous and nonaqueous solvents at ambient temperatures [3–6]. In view of the significant advantages available with the RRDE technique, it is perhaps surprising that relatively few applications have been reported in high temperature molten salt electrolytes.

A critical feature in the design of an RRDE for use in high temperature fluoride electrolytes is finding a suitable combination of electrode and insulator materials with the necessary thermal, electrochemical and corrosion properties. A limited range of electrode materials, such as tungsten, gold, platinum, nickel and various forms of carbon, has been successfully employed in cryolite and sodium fluoride melts [7–10]. The selection of a suitable insulator material is more restricted, with boron nitride being the only established material available for this type of application. Although the rotating disc electrode (RDE) has been previously used for studies in cryolite melts [11–14], applications involving the RRDE have been limited to lower temperature molten salt electrolytes up to 450 °C [15–17]. The development of an RRDE that could be used at higher temperatures may provide a powerful tool for the detection of short-lived intermediate species involved, for example, in the aluminium electrodeposition process in molten cryolite [18, 19].

In the present work, construction and performance details of a compact gold–molybdenum RRDE are described. The operation of the RRDE was evaluated in different melt compositions in terms of parameters such as thermal stability, sensitivity, reproducibility and mechanical performance. Preliminary studies have shown that the RRDE should be useful for elucidating details about the electrochemical behaviour of chemical species in cryolite-based electrolytes at temperatures up to 1000 °C and rotation rates between 0 and 2000 rpm.

2. Experimental details

2.1. *Design and construction of the rotating ring-disc electrode*

The design and general construction of a high temperature RRDE are shown in Fig. 1. Molybdenum (99.95%, Metallwerk Plansee GmbH) was used as the disc material because of its superior machining properties relative to tungsten. High purity gold (99.9%, Johnson Matthey (Aust.) Ltd.) was used as the ring material because of its stability and ability to induce electrode reactions at high temperatures.

* Author to whom correspondence should be addressed.

0021-891X 1995 Chapman & Hall

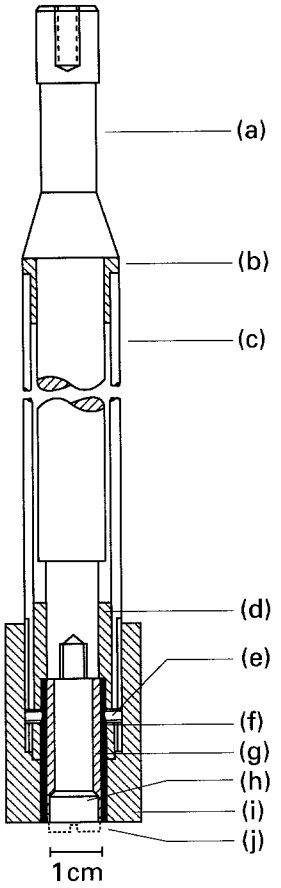

Fig. 1. A schematic diagram of the rotating ring-disc electrode: (a) internal Inconel shaft/rotator connection, (b) glass-filled Teflon bush, (c) outer Inconel tube, (d) boron nitride support, (e) stainless steel screws, (f) gold tube, (g) boron nitride gap insulator, (h) molybdenum rod, (i) outer boron nitride insulating sheath and (j) slotted end-piece.

The insulating gap material consisted of either hot pressed boron nitride (Union Carbide Corporation, HBR Grade) or pyrolytic boron nitride (Advanced Ceramics Corp., PBN Coating on Graphite). Boron nitride was selected because of its thermal stability, chemical resistance to cryolite, machining properties and low coefficient of thermal expansion ($2.0 \times 10^{-6}\,°C^{-1}$ at 1200 °C (HBR) [20] and $2.6 \times 10^{-6}\,°C^{-1}$ at 1100 °C (PBN) [21]) compared to other ceramic materials.

The fabrication process involved firstly press-fitting a 25 mm long solid boron nitride rod (nominal diameter 11 mm) into a pre-fabricated gold tube (nominally 11 mm i.d. × 13 mm o.d. × 25 mm long). The boron nitride was then progressively drilled to give a counter-bored finish with an internal diameter stepped from 8 to 10 mm (working end). A stepped molybdenum rod of 8–10 mm diameter was machined with a slotted end-piece at the larger diameter end. The rod was then threaded at the smaller diameter end and inserted into the boron nitride-sleeved gold tube to form a liquid-tight seal. The entire assembly was then screwed onto an Inconel 600 shaft (13.5 mm diameter × 60 cm long), the end of which had been machined to suit the electrode rotator; this provided the electrical contact to the molybdenum disc. Inconel was chosen because of its resistance to fluoride vapour as well as its thermal strength at high temperatures. An outer Inconel tube (16 mm i.d. × 19 mm o.d. × 55 cm long) was then pressed into position over a glass-filled Teflon bush located near the top of the Inconel shaft, and a boron nitride support was inserted near the ring-disc assembly to ensure separation of the inner shaft and outer Inconel tube. It was possible to use glass-filled Teflon with its excellent electrical insulation, mechanical and machining properties because heat resistance was not critical. Two small stainless steel screws were inserted directly through the outer Inconel tube and boron nitride support into the gold tube to provide electrical contact to the gold ring. These screws were machined flush to allow a thread to be cut on the outer Inconel tube so that an outer boron nitride insulating sheath could be screwed over the entire ring-disc assembly. The electrode face was machined flush removing the slotted end-piece, ensuring that the ring and disc were coplanar, and finished with grade P800 emery paper using alcohol as the lubricant. Electrical contacts were made via carbon brushes spring-loaded onto the inner Inconel shaft and outer Inconel tube.

The dimensions of the Au–Mo RRDE were: disc radius (r_1) = 0.50 cm, ring inner radius (r_2) = 0.55 cm, ring outer radius (r_3) = 0.65 cm, disc area: 0.79 cm^2, and ring area: 0.38 cm^2. The theoretical collection efficiency of an RRDE with these dimensions is 30.92% [6]. Gold–gold and gold–graphite RRDEs with similar dimensions to the above electrode have also been constructed for related studies. A photograph of typical Au–Mo RRDEs is shown in Fig. 2.

2.2. *Electrochemical instrumentation and laboratory cell*

A bipotentiostat (Pine Instrument Company, Model AFRDE4) was used to independently control the potential of the ring and disc electrodes. An electrode rotator (Pine Instrument Company, Model AFASRE) was used to control the rotation of the RRDE. Current–voltage traces were recorded on a YEW Type 3086 *x–y* recorder (Yokogawa Hokushin Electric, Japan). Preliminary studies on electrode materials were performed using a Model 273 potentiostat/galvanostat with Model 270 electrochemical analysis software (EG&G PAR Corp., USA).

The electrochemical cell was constructed from graphite (Morganite, CS Grade) with dimensions 90 mm i.d. × 110 mm o.d. × 140 mm long and supported within an Inconel 600 furnace tube. The RRDE was inserted into the cell through a water-cooled seal on the head of the furnace tube. The furnace (A. J. Wilcock Scientific & Engineering Equipment, Australia, model 5V-4T) was equipped with a temperature controller (Eurotherm series 70) and programmer (Eurotherm type 125). The cell temperature was raised at 1 °C per minute and allowed to equilibrate for at least one hour after reaching its working temperature. The melt temperature was measured

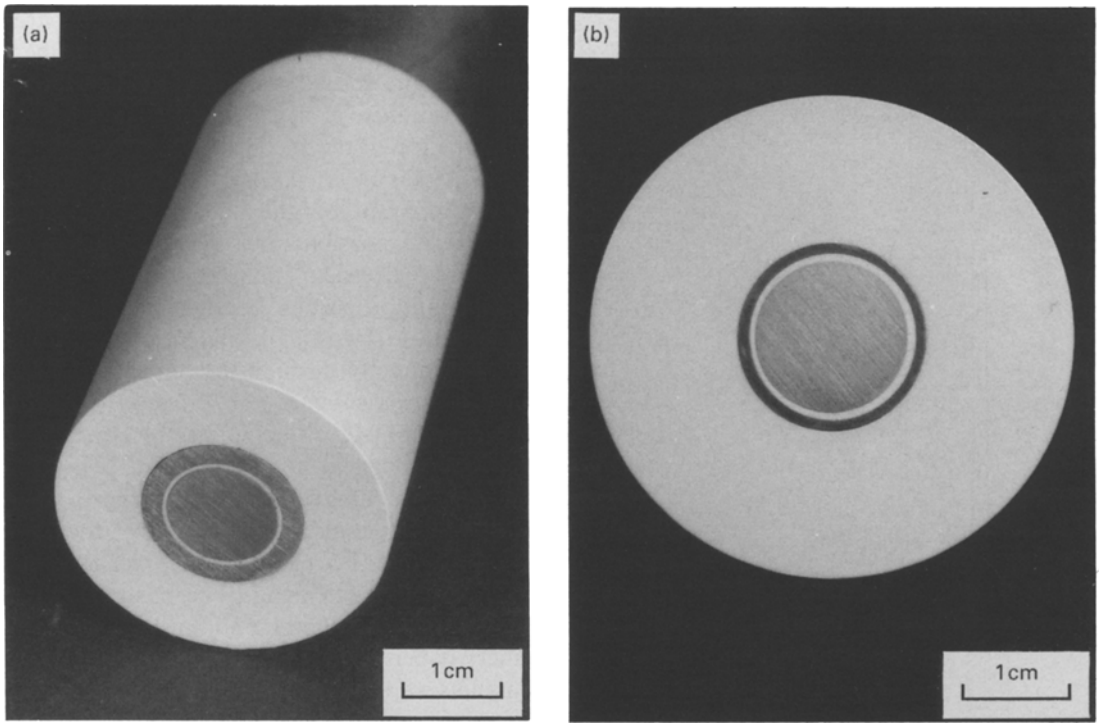

Fig. 2. A photograph of typical high temperature Au–Mo RRDEs: (a) $r_1 = 0.4$ cm, $r_2 = 0.44$ cm, $r_3 = 0.58$ cm and (b) $r_1 = 0.4$ cm, $r_2 = 0.44$ cm, $r_3 = 0.495$ cm.

with a type K chromel–alumel thermocouple. A continuous stream of argon was passed through the furnace tube and over the electrochemical cell to minimise oxidation of the graphite cell components.

Electrochemical measurements were performed using either a Au RDE or a Au–Mo RRDE as the working electrode(s), the graphite cell as the counter electrode and an aluminium/cryolite reference electrode similar in design to that described by Burgman *et al.* [22]. Synthetic cryolite (Na_3AlF_6) and alumina (courtesy Comalco Research Centre, Melbourne, Australia), aluminium fluoride (99.9% CERAC Inc.), and calcium fluoride (99.9% Aldrich Chemical Co. Inc.) were dried under vacuum at 120 °C for 4 h and subsequently stored under vacuum until required. The various melt components (~ 450 g) were premixed prior to being introduced into the graphite cell. All other chemicals were usually of analytical grade purity, and were added to the melt as either the oxide or fluoride salt, in the form of a preweighed pellet which had been dried and stored in a desiccator prior to use. Electrochemical measurements were made at bath ratios (*BR*, defined as the mass ratio of NaF/AlF_3) between 1.5 and 1.0, and at working temperatures of between 10–15 °C above the liquidus temperature of the melt.

3. Results and discussion

3.1. *Rotating disc voltammetry in cryolite-based melts*

Cyclic voltammetry was used to assess and characterize the behaviour of electrode materials such as molybdenum, gold, nickel, graphite and glassy carbon for use in the construction of an RRDE. These studies identified molybdenum as being the most suitable disc substrate for cathodic measurements involving the deposition of aluminium metal from cryolite because of its high melting point and the ability to form a stable aluminium film. The solubility of molybdenum in aluminium is very low at 1000 °C [23] and so minimal interference with the aluminium deposition process occurs at more negative electrode potentials. As expected, graphite and glassy carbon were both well suited to studies involving anode gas evolution at positive electrode potentials, the former material being chosen because of its superior machining properties. Furthermore, gold appeared to be a potentially useful ring substrate because of low residual background current and an ability to induce electrochemical reactions over a range of working potentials.

In view of the paucity of information available on the voltammetry of electroactive species in cryolite-based melts, there was a need to find a suitable redox system that could be used to assess the performance of the Au RDE. Cyclic voltammograms for reduction of Mn^{2+} and Fe^{2+} using a gold wire electrode have previously been reported in cryolite at 1015 °C [13, 24]. Figure 3 shows a cyclic voltammogram at a stationary Au RDE for reduction of 0.1 M Mn^{2+} (MnF_2) to Mn in a bath consisting of 80 wt % cryolite, 10 wt % alumina and 10 wt % aluminium fluoride at 960 °C ($BR = 1.14$). At high electrode currents the voltammograms were recorded using *iR* compensation to allow accurate potential measurements. Under fast scan rate conditions (> 1000 $mV\,s^{-1}$), well defined peaks were observed on both the forward and reverse scans, consistent with behaviour expected for an

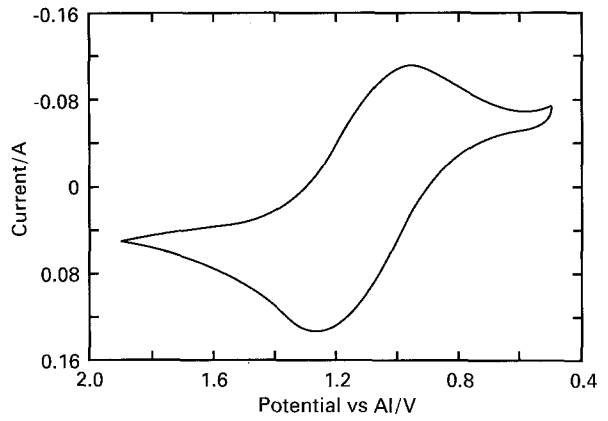

Fig. 3. A cyclic voltammogram at a *stationary* Au RDE (area: 0.20 cm^2) for reduction of 0.1 M Mn^{2+} in a bath of 80 wt % cryolite, 10 wt % alumina and 10 wt % aluminium fluoride at 960 °C ($BR = 1.14$), iR compensation: 0.5 Ω and potential scan rate: 1000 mV s^{-1}.

electrochemically reversible diffusion controlled process. Additionally, the values for the reduction peak current and oxidation peak current were similar in magnitude, suggesting that the system is also chemically reversible without any apparent complications from surface-related phenomena. The data confirm that the Mn^{2+}/Mn system should be useful for RDE measurements in cryolite-based melts.

The operating performance of the Au RDE was evaluated by determining the diffusion coefficient for Mn^{2+} in pure cryolite at 1014 °C from the slope of a plot of the mass transport limited faradaic current against the square root of the rotational velocity, according to the Levich equation [25],

$$i_l = 0.62nFAD^{2/3}\nu^{-1/6}\omega^{1/2}C \quad (1)$$

$$D = \left[\frac{di_L}{d\omega^{1/2}}\frac{\nu^{1/6}}{0.62nFC}\right]^{3/2} \quad (2)$$

where i_l is the limiting current (A), i_L is the limiting current density (A cm^{-2}), A is the electrode area (cm^2), ω is the rotation rate (rad s^{-1}), ν is the kinematic viscosity of molten cryolite at 1015 °C (0.011 cm^2 s^{-1}), C is the bulk concentration (1.04×10^{-4} mol cm^{-3}), D is the diffusion coefficient

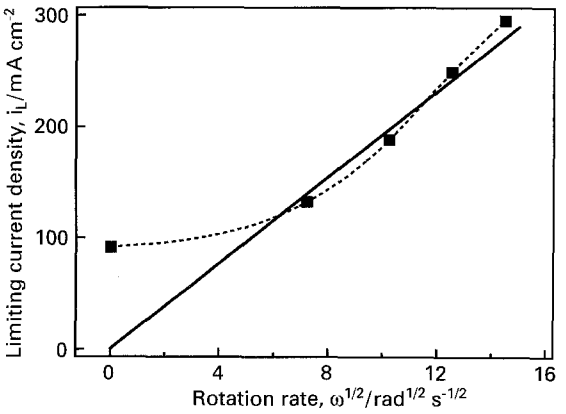

Fig. 4. Levich plot of limiting current density (i_L) as a function of rotation rate ($\omega^{1/2}$) for reduction of 0.1 M Mn^{2+} at a Au RDE (area: 0.20 cm^2) in pure cryolite at 1014 °C.

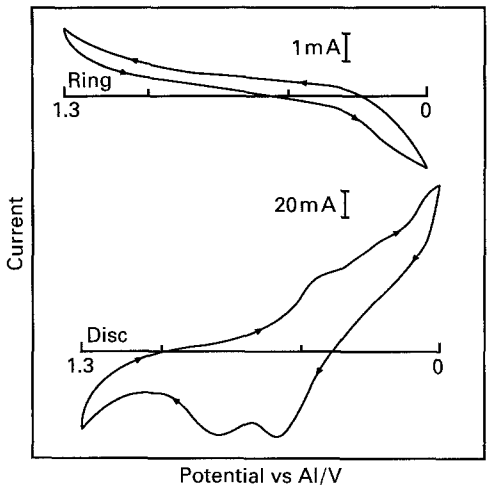

Fig. 5. Typical disc current–disc potential and ring current-disc potential curves obtained at a *stationary* Au–Mo RRDE ($r_1 = 0.5$ cm, $r_2 = 0.55$ cm, $r_3 = 0.65$ cm, disc area: 0.79 cm^2, and ring area: 0.38 cm^2) in a bath of 76.7 wt % cryolite, 3 wt % alumina, 15.3 wt % aluminium fluoride and 5 wt % calcium fluoride at 948 °C ($BR = 1.0$). Ring potential: 1.0 V and potential scan rate: 50 mV s^{-1}.

(cm^2 s^{-1}), n is the number of electrons transferred ($n = 2$), and F is the Faraday constant. Figure 4 shows the variation of limiting current density with rotation rate ($\omega^{1/2}$) for reduction of 0.1 M Mn^{2+} at a Au RDE in pure cryolite at 1014° C. Although a linear response is observed at high rotation rates, natural convection causes i_L to be significantly greater than values predicted by theory at low rotation rates. This phenomenon limits the applicability of the Levich equation at these temperatures to rotation rates of above approximately 400 rpm. A least squares analysis of the linear portion of the plot of i_L against $\omega^{1/2}$ yielded a slope of 0.0187 A cm^{-2} - $rad^{-1/2}$ $s^{1/2}$; this value was independent of potential scan rate. Under these conditions a value of 1.89×10^{-5} cm^2 s^{-1} was obtained for the diffusion coefficient of Mn^{2+} in molten cryolite, which is slightly lower than values previously reported (3×10^{-5} cm^2 s^{-1} and 4×10^{-5} cm^2 s^{-1} [13, 24]).

3.2. *Rotating ring-disc voltammetry in cryolite-based melts*

A gold ring and a molybdenum disc were chosen as a potentially useful combination for the application of the ring-disc technique in high temperature cryolite-based melts. Molybdenum exhibits a relatively low background current over a wide potential range, while specific interactions at the gold ring limit its effective working range to between 0.7 and 1.6 V versus an aluminium reference electrode. Figure 5 shows typical voltammograms obtained at a *stationary* Au–Mo RRDE in a bath consisting of 76.7 wt % cryolite, 3 wt % alumina, 15.3 wt % aluminium fluoride and 5 wt % calcium fluoride at 948 °C ($BR = 1.0$), as a result of scanning the disc potential while maintaining the ring potential at 1.0 V. The disc current–disc potential curve on the forward potential scan is characterized by a series of small

waves prior to the onset of the aluminium deposition reaction which are attributed to the formation of a number of Mo–Al alloys [23]. A series of waves was observed during the reverse potential scan which are presumably related to aluminium being stripped from the various alloy phases. The peak heights for the various anodic processes on the reverse scan were examined as a function of deposition time and reversing potential. The peak height for all processes increased with an increase in holding time at a fixed deposition potential. Similarly, an increase in peak height was observed as the reversing potential was made more negative. Both these observations support the above conclusion of alloy formation. In contrast, the corresponding ring current–disc potential curve exhibits a relatively stable background prior to the onset of an anodic wave, at a potential coinciding with the aluminium electrodeposition process at the disc. These results suggest that the Au–Mo RRDE may be a useful tool for elucidating details about electrochemical reaction mechanisms in cryolite-based melts.

An RRDE is usually calibrated by determining its collection efficiency (N), defined as the fraction of species produced at the disc electrode which is capable of reacting at the ring electrode [3]. Theoretical and experimental values for N can be readily compared provided a suitable redox system is available, ideally a system where both the oxidised and reduced forms of the electroactive species are soluble. The oxidation of ferrocene (bis-cyclopentadienyl iron) and reduction of ferricyanide are often used as model systems in organic and aqueous solvents, but no useful redox system has been established for work in cryolite-based melts. The voltammetric behaviour of chemical species such as FeF_3, MnO_2, CrF_3, V_2O_5, Ta_2O_5 and Nb_2O_5 was examined in various cryolite-based melts using a Au–Au RRDE at rotation rates between 0 and 2000 rpm. Unfortunately, no redox couple suitable for use as a model system could be found in the potential range available at the gold ring. It should be stressed, however, that these results do not necessarily imply that the redox systems investigated are not electrochemically active in molten salt electrolytes.

An alternative approach, based on measurements involving the dissolution of the molybdenum disc surface and subsequent detection of soluble species at the ring, was used to determine the N of the Au–Mo RRDE. Figure 6(a) shows a typical voltammogram obtained at a *stationary* Au–Mo RRDE in a bath consisting of 80 wt % cryolite, 10 wt % alumina and 10 wt % aluminium fluoride at 960 °C ($BR = 1.14$), as a result of scanning the disc potential in the positive direction while maintaining the ring potential at 0.8 V. The disc current–disc potential curve is characterized by a large single anodic wave resulting from direct oxidation of the molybdenum disc surface, and a corresponding cathodic wave resulting from the reduction of products formed at the disc surface. The height of both the oxidation and reduction waves

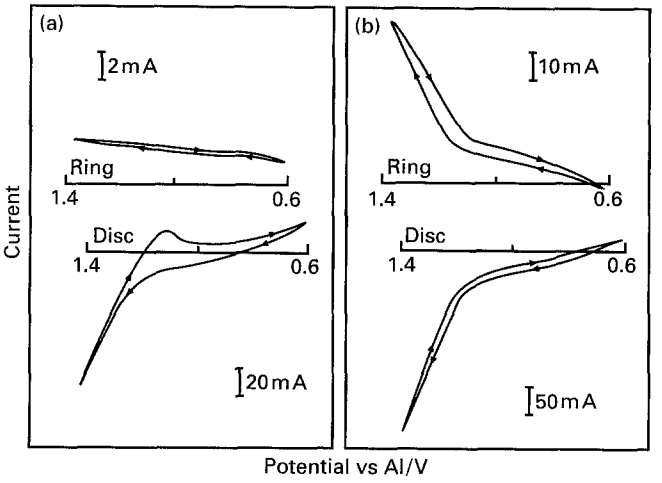

Fig. 6. Typical disc current–disc potential and ring current-disc potential curves obtained at a Au–Mo RRDE ($r_1 = 0.5$ cm, $r_2 = 0.55$ cm, $r_3 = 0.65$ cm, disc area: 0.79 cm^2, and ring area: 0.38 cm^2) in a bath of 80 wt % cryolite, 10 wt % alumina and 10 wt % aluminium fluoride at 960 °C ($BR = 1.14$). (a) Stationary electrode, ring potential: 0.8 V and potential scan rate: 50 mV s^{-1}. (b) Rotation rate: 1500 rpm, ring potential: 0.8 V and potential scan rate: 50 mV s^{-1}.

was dependent on the reversing potential applied at the disc during the forward potential scan. Under these conditions, no response was observed at the gold ring, indicating that the reaction products formed at the surface of the molybdenum disc were not being transported to the ring.

Figure 6(b) shows current–voltage curves obtained at the Au–Mo RRDE at a rotation rate of 1500 rpm. A significant increase in wave height is observed at the molybdenum disc during the forward potential scan, while the cathodic wave observed previously on the reverse potential scan at the stationary molybdenum disc is no longer visible. Importantly, a single well defined cathodic wave is now observed at the gold ring, as shown by the ring current–disc potential curve. Under convective mass transport control, the soluble species formed at the molybdenum disc is transported to, and subsequently detected at, the gold ring. From the available data, it is possible to calculate a value for N from the ratio of the ring electrode current (i_R) to disc electrode current (i_D), according to the following equation,

$$N = \frac{i_R n_D}{i_D n_R} \tag{3}$$

where n_D and n_R are the number of electrons transferred on the disc and ring, respectively [4].

The collection efficiency of the Au–Mo RRDE at a rotation rate of 1500 rpm, assuming n_D and n_R are equal, was calculated to be 19.7%, compared to the theoretical value of 30.92% determined from the geometry of the electrode [6]. The difference between the observed and theoretical collection efficiencies may be attributed to different values for n_D and n_R, or to the presence of a surface controlled reaction at the disc causing erroneous values to be obtained for the mass transport controlled faradaic current.

Experimentally measured values of N were found to be slightly dependent on the rotation rate of the electrode, which is consistent with behaviour expected for a more complex mechanism than one involving only convective diffusion. Additionally, N can vary significantly with rotation rate depending upon the degree of noncoplanarity that exists between the ring and disc [6]. It is possible to determine the contribution of a surface controlled process to the total faradaic current from the general expression [6],

$$\frac{1}{i} = \frac{1}{i_{surf}} + \frac{1}{B\omega^{1/2}} \quad (4)$$

where i is the total current density, i_{surf} is the surface controlled current density and $B\omega^{1/2}$ $(= i_L)$ is the mass-transport controlled current density, provided a plot of $1/i$ against $1/\omega^{1/2}$ is linear. The present data does not fit Equation 4, which implies that additional factors are operating.

It has been well documented [26] that a noncoplanar ring–disc configuration can lead to discrepancies in measured N values. One would expect a degree of noncoplanarity to exist when the ring–disc assembly is operating at temperatures around 1000 °C, given the differences between the thermal expansion coefficients of the electrode and insulator materials. A detailed examination of the Au–Mo RRDE assembly, after removal from the melt, has revealed ring-disc plane misalignments of up to 0.4 mm. Assuming such a misalignment exists at the working temperature, then using an estimate based on the data of [26] for an RRDE with $r_1 = 1.5$ mm, $r_2 = 2.5$ mm, $r_3 = 4.5$ mm, one could expect N to decrease by around 25%. The difference between the observed and the theoretical N values for the Au–Mo RRDE was of a similar order, suggesting that noncoplanarity is the most likely cause of non-ideal behaviour in high temperature melts.

4. Conclusions

A Au–Mo RRDE has been developed for high temperature electrochemical studies in cryolite-based melts. The electrode allows electrochemical measurements to be made in various melt compositions for experimental times of up to 3 h, at temperatures of around 100 °C and at rotation rates between 0 and 2000 rpm. A detailed examination of the electrode after disassembly revealed no visible melt leakage at the ring-insulator and disc-insulator interfaces. The operating performance of the RRDE was evaluated directly from measurements involving the dissolution of the disc surface and detection of soluble species transported to the ring. The Au–Mo RRDE displayed a collection efficiency less than the expected theoretical value determined from the geometry of the electrode. This behaviour was primarily attributed to noncoplanarity of the electrode surface as a result of the different expansion rates of the various materials at the working temperature of 960 °C. This work suggests that the RRDE should be a highly sensitive and specific technique for mechanistic or related studies in cryolite-based melts. The advantages offered by the RRDE should extend the scope of electrochemical investigations in high temperature molten salt electrolytes, complementing the more established techniques that are currently available.

Acknowledgments

The authors wish to acknowledge A. M. Vecchio-Sadus for advice on melt compositions and preparations, and R. L. Deutscher and D. C. Constable for helpful comments on the manuscript. Thanks are also due to Comalco Research Centre (Melbourne) for supply of melt materials.

References

[1] D. G. Lovering and R. J. Gale (eds), 'Molten Salt Techniques', vol. 1, Plenum Press, New York (1983).
[2] D. L. Manning and G. Mamantov, *in* 'Characterization of Solutes in Nonaqueous Solvents', (edited by G. Mamantov), Plenum Press, New York (1978).
[3] W. J. Albery and M. L. Hitchman, 'Ring-Disc Electrodes', Oxford University Press, Oxford (1971).
[4] W. J. Albery and S. Bruckenstein, *Trans. Faraday Soc.* **62** (1966) 1920.
[5] S. Bruckenstein and B. Miller, *Acc. Chem. Res.* **10** (1977) 54.
[6] F. Opekar and P. Beran, *J. Electroanal. Chem. Interfacial Electrochem.* **69** (1976) 1.
[7] D. L. Manning and G. Mamantov, *High Temp. Sci.* **8** (1976) 219.
[8] K. A. Bowman, Doctoral Dissertation, University of Tennessee, Knoxville (1977).
[9] J. J. Duruz, G. Stehle and D.Landolt, *Electrochim. Acta* **26** (1981) 771.
[10] E. Y. L. Sum and M. Skyllas-Kazacos, *ibid.* **36** (1991) 31.
[11] E. W. Dewing and K. Yoshida, *Can. Met. Quart.* **15** (1976) 299.
[12] J. J. Del Campo, J. P. Millet and M. Rolin, *Electrochim. Acta* **26** (1981) 59.
[13] J. M. Tellenbach and D. Landolt, *ibid.* **33** (1988) 221.
[14] J. W. Burgman and P. J. Sides, *ibid.* **34** (1989) 841.
[15] J. Phillips, R. J. Gale, R. G. Wier and R. A. Osteryoung, *Anal. Chem.* **48** (1976) 1266.
[16] S. Takahashi and N. Koura, *J. Electroanal. Chem. Interfacial Electrochem.* **188** (1985) 245.
[17] H. Yabe, K. Ema and Y. Ito, *Electrochim. Acta* **34** (1989) 1479.
[18] J. J. Duruz and D. Landolt, *J. Appl. Electrochem.* **15** (1985) 393.
[19] J. M. Tellenbach and D. Landolt, *J. Appl. Electrochem.* **18** (1988) 639.
[20] UCAR Boron Nitride, Union Carbide Corporation, SP1001 Rev. 5M1086 (1985).
[21] BORALLOY Pyrolytic Boron Nitride, Union Carbide Coatings Service Corporation, CP-4779 Rev.3 5M 8/90 (1987).
[22] J. W. Burgman, J. A. Leistra and P. J. Sides, *J. Electrochem. Soc.* **133** (1986) 496.
[23] M. Hansen and K. Anderko, 'Constitution of Binary Alloys', 2nd edn, McGraw-Hill, New York (1958).
[24] G. Stehle, J. J. Duruz and D. Landolt, *J. Appl. Electrochem.* **12** (1982) 591.
[25] V. G. Levich, 'Physicochemical Hydrodynamics', Prentice-Hall, Englewood Cliffs, New Jersey, (1962).
[26] W. Kennedy and H. Linge, *Rev. Sci. Instrum.* **54** (1983) 361.